Fast multigrid fluorescent ion chamber with 0.1 ms time response

Motohiro Suzuki,[a]* Naomi Kawamura,[a] Farrel W. Lytle[b] and Tetsuya Ishikawa[a,c]

[a]SPring-8/JASRI, 1-1-1 Kouto, Sayo, Mikazuki, Hyogo 679-5198, Japan, [b]The EXAFS Company, HC 74 Box 236, Eagle Valley Road, Pioche, NV 89043, USA, and [c]SPring-8/RIKEN, 1-1-1 Kouto, Sayo, Mikazuki, Hyogo 679-5148, Japan. E-mail: m-suzuki@spring8.or.jp

A fast multigrid ion chamber for the detection of fluorescent X-rays has been developed. The structure of 17 grids with close separation was employed to maximize the time response as well as to give sufficient detection efficiency. The measured rise/fall response time to cyclic X-rays was shorter than that of an existing three-grid ion chamber by more than one order of magnitude. A 0.13 ms time response was obtained at the 500 V applied voltage, where the detector can stably operate without any discharge. The available frequency range is as high as 1 kHz with a practical amplitude response.

Keywords: ion chamber detectors; spectroscopy; fluorescent XAFS/XMCD; modulation techniques; helicity modulation.

1. Introduction

The recent development of X-ray modulation spectroscopy (Suzuki *et al.*, 1998, 2000, 2001) has significantly improved the signal-to-noise ratio in X-ray magnetic circular dichroism (XMCD) measurements. The helicity-modulation technique (Suzuki *et al.*, 1998, 1999) gives, in a shorter measuring time, extremely high-quality XMCD spectra that enable us to discuss fine structures of the order of 10^{-4}. The temperature (Maruyama, 2001; Uemoto *et al.*, 2001) or the sample-composition (Kawamura *et al.*, 2001) dependence of XMCD has become achievable in a practical measuring time.

The modulation technique is well adapted to the X-ray absorption measurements in a transmission geometry using two conventional ion chambers with parallel plane electrodes. Extension of the modulation spectroscopy to fluorescent X-ray measurements will allow us to investigate diluted magnetic materials as well as single/multilayer systems on X-ray opaque substrates by means of XMCD. However, currently available fluorescent X-ray detectors do not have sufficiently fast time response, being incompatible with the modulation technique (typically at 40 Hz). A three-grid fluorescent ion chamber (Stern & Heald, 1979; Lytle *et al.*, 1984) supplied from The EXAFS Company is widely used for fluorescent XAFS/XMCD measurements. Despite its high performance in a static operation, such as large aperture for fluorescent X-rays, low dark current and high stability, the time response of the detector is too slow to follow the incident X-rays modulated at several tens of Hz. If the detector was improved to have a faster time response, it would be better suited to the fluorescent X-ray measurement in modulation mode.

One of the key parameters that determine the time response of the ion chamber is the electric field between the electrode grids: a higher electric field gives a faster response. The higher electric field can be realised by narrowing the separation between the grids. The number of grids should be increased to give sufficient absorption length of fill gas and to conserve the efficiency of the detector. In addition, the detector should operate with the applied voltage as high as possible. Some special manufacturing processes are needed to avoid any discharge that causes the transient noise within the detector.

Table 1
Parameters of three-grid and multigrid ion chamber detectors.

	Three-grid detector	Multigrid detector
Number of grids (collector + spacer)	3 (1 + 2)	17 (8 + 9)
Separation of grids (mm)	17	5
Collector grid material	Ni mesh	Aluminized Mylar
Window aperture (mm)	86 (diameter)	77 × 77
Discharge voltage (full of Ar) (V)	200	550
Electric field (kV m^{-1})†	8.8	100
Rise/fall time (ms)†	4.5	0.13

† With 150 V applied for three-grid detector and 500 V for multigrid detector.

By including the modifications above, we have built a new 17-grid fluorescent X-ray ion chamber of faster response. The rise/fall response time of this multigrid detector was measured using X-rays from synchrotron radiation and compared with that of an existing three-grid ion chamber. The response time of the multigrid detector was more than one order of magnitude faster than that of the three-grid detector. The frequency response curve was estimated from the measured rise/fall time.

2. Design and construction of the multigrid ion chamber

The design target of the new multigrid ion chamber was to have the time response fast enough to follow cyclic X-rays at several tens of Hz. For this aim, the electric field between the grids was optimized and transient discharges within the detector were minimized. In Table 1 the design parameters of the multigrid detector are compared with those of an existing three-grid detector, together with the measured rise/fall time, which will be described in §4.

Fig. 1 shows the grid structure of the multigrid detector. The new detector has eight collector grids and nine spacer grids. Both the

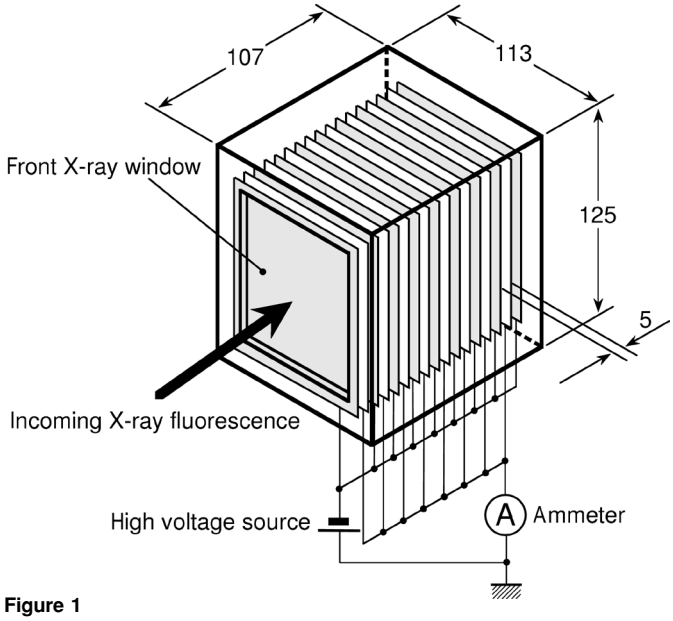

Figure 1
A schematic diagram of the multigrid fluorescent ion chamber. The skeleton frame shows the detector body. Both the spacer (grey) and the collector (white) grids are made of X-ray-transparent Mylar sheets. The units for the dimensions are mm.

collector and the spacer grids are made of X-ray-transparent 6 μm Mylar sheets aluminized on both sides of thickness 500 nm. The opening size of the front X-ray window (the first spacer grid) is the same as that of the existing fluorescent ion chambers. The separation between the grids is 5 mm, which is 3.4 times closer than in the three-grid detector with a 17 mm separation. With the closer grid separation the response time of the detector should be shorter than that of the three-grid detector. These 17 grids result in an effective ion chamber depth approximately the same as that with the existing five-grid unit, 80 mm. For high-energy fluorescent X-rays, the total absorption by the 17 grids is much less than by a fill gas such as Ar. Each collector or spacer grid can be separately activated by making a connection to the appropriate grids. This allows the use of a smaller number of grids, which is particularly useful for softer X-rays minimizing unwanted absorption by the grids as well as some leakage current or electrical noise. The detector has been assembled with care to minimize sharp points on the screws used to hold the grid frames together. The aluminium frames and brass screws are totally covered by a Delrin frame, which is a much better insulator than the Teflon used in the existing detectors. These modifications allowed stable operation at higher voltages than previous EXAFS Company detectors.

3. Experimental

Output waveforms for the input square-wave cyclic X-rays were used for the evaluation of the time response of both the new multigrid detector and the existing three-grid detector. The input cyclic X-rays were prepared using fluorescent X-rays from a Cu plate (0.1 mm-thick) irradiated by chopped monochromatic X-rays (E = 8998 eV, 10 eV above the absorption threshold of the Cu K-edge). A mechanical chopper made of four brass blades (0.7 mm-thick) was placed upstream of an I_0 monitor ion chamber to produce a square wave of X-ray intensity with almost 100% duty cycle. Owing to the different time response between the detectors, the chopping frequency was set to 10 Hz for the three-grid detector and to 100 Hz for the multigrid detector. In order to keep the detection stable, a constant flow of Ar (N_2) gas was supplied to the fluorescent (I_0) ion chamber during the measurement. The measurements were performed at undulator beamline BL39XU of SPring-8 using the set-up shown in Fig. 2.

The output waveform dependence on the applied voltage was measured for both fluorescent ion chambers. To record the output waveforms, the output current of the ion chamber was amplified and converted to a voltage signal using a current amplifier (Keithley 428, 10^8 V/A gain, no filter), then digitized with an analog–digital converter (National Instruments PCI-MIO-16XE-50) at a 50 μs sampling rate to store in computer memories.

4. Performance of the multigrid detector

The dependence of the output waveform on the applied voltage is shown in Fig. 3(*a*) for the three-grid chamber, and in Fig. 3(*b*) for the multigrid chamber with all the collector and the spacer grids enabled. The vertical scale plots the output voltage of the current amplifier. Data averaged for ten periods are displayed. The measured output response shows a two-stage process: the faster time response corresponds to the drift of the electrons between grids, and the slower response is due to the positive ions. The waveforms show a time structure typical of the transient response of a conventional ion chamber (Knoll, 1989). Consideration of only the slower process is sufficient to evaluate the practical time response of the detector. For this purpose the equivalent circuit of an RC low-pass filter gives a good approximation of an ion chamber operated in a cyclic mode. Then, the time responses, $R_r(t)$ for the rising edge and $R_f(t)$ for the falling edge, are represented as

$$R_r(t) = R_r(\infty)\left[1 - \exp(-t/\tau_r)\right], \quad (1)$$

$$R_f(t) = R_f(0)\exp(-t/\tau_f), \quad (2)$$

where t is the time after the beam is turned on/off, $R_r(\infty)$ is the output expected for d.c. input, and $R_f(0)$ is the output when the beam has just been turned off. The rise and fall times (τ_r and τ_f, respectively) are functions of the applied voltage. They were evaluated for each applied voltage through a least-squares fit of the output waveforms to equations (1) or (2).

Fig. 4 shows the rise time τ_r as a function of the applied voltage. The result for the three-grid ion chamber is displayed by the open circles, and the closed circles are for that of the multigrid chamber. The data points include the correction for the 40 μs output rise time of the current amplifier. This contribution was at most 7% for the multigrid detector at 650 V. The error bars on the markers show the standard deviation resulting from the least-squares fit. The rise time

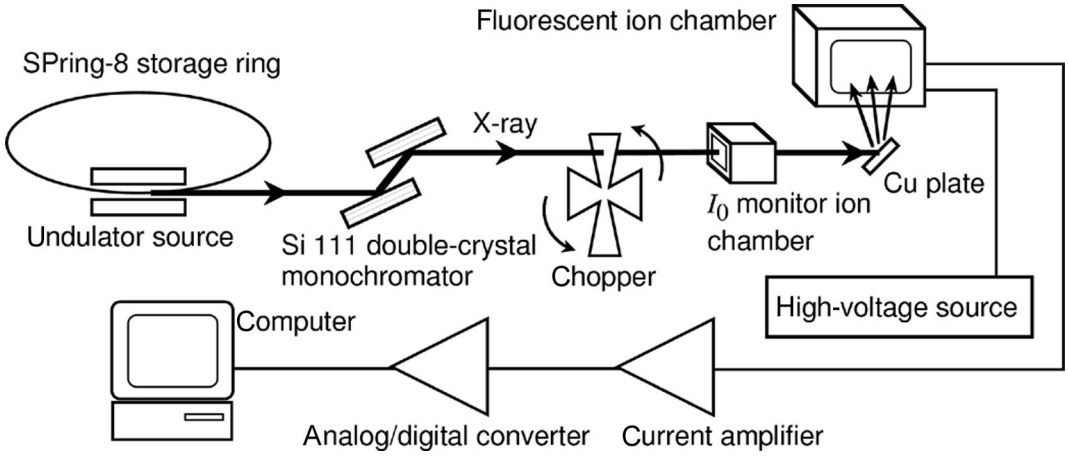

Figure 2
Set-up for the measurement of the time response of fluorescent ion chambers.

of the new multigrid detector is ten times shorter than that of the three-grid detector when the same voltage is applied.

For both the three-grid and the multigrid detector we found a log-linear response of the rise/fall time *versus* the applied voltage, V. The best-fit functions are tabulated in Table 2 and are also shown by the solid lines in Fig. 4. A similar dependence of the rise and the fall time was obtained for both the three-grid and the multigrid chamber.

In addition to the ten-times faster response at the same applied voltage, the multigrid detector shows high stability at higher voltage. No transient noise was observed up to 500 V, in contrast with the three-grid detector which was found to be noisy above 200 V. Therefore, the practical rise/fall time of the three-grid detector is limited to 3.5 ms, whereas the multigrid detector can operate with the rise/fall time as fast as 0.1 ms at a higher applied voltage.

The frequency response of the multigrid detector was estimated from the measured rise/fall time using a function giving the response of an RC low-pass filter,

$$F(f) = \left[1 + (2\pi f \tau)^2\right]^{-1/2}, \qquad (3)$$

where f is the frequency and τ is the rise/fall time of the ion chamber. The plots in Fig. 5 are the response curves for τ = 15, 1.2, 1.3 and 0.13 ms, corresponding to the three-grid detector used at 50 and 500 V and the multigrid detector used at 50 and 500 V, respectively.

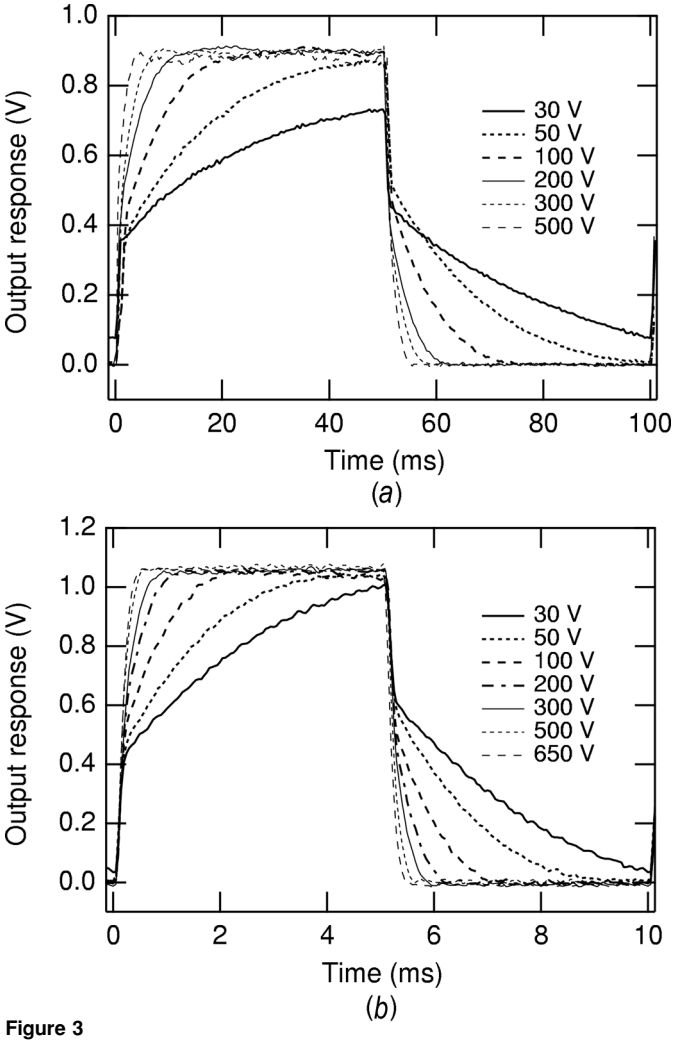

Figure 3
(*a*) The output waveforms of an existing three-grid fluorescent ion chamber at the different applied voltages. The incident fluorescent X-rays were chopped into a square wave at 10 Hz. (*b*) The output waveforms of the new multigrid ion chamber to the incident X-rays at 100 Hz, displayed in the reduced time scale.

Table 2
Response time of the three-grid/multigrid ion chambers.

Detector	τ_r (ms)	τ_f (ms)
Three-grid	$940\ V^{-1.07}$	$960\ V^{-1.07}$
Multigrid	$65\ V^{-1.01}$	$71\ V^{-1.02}$

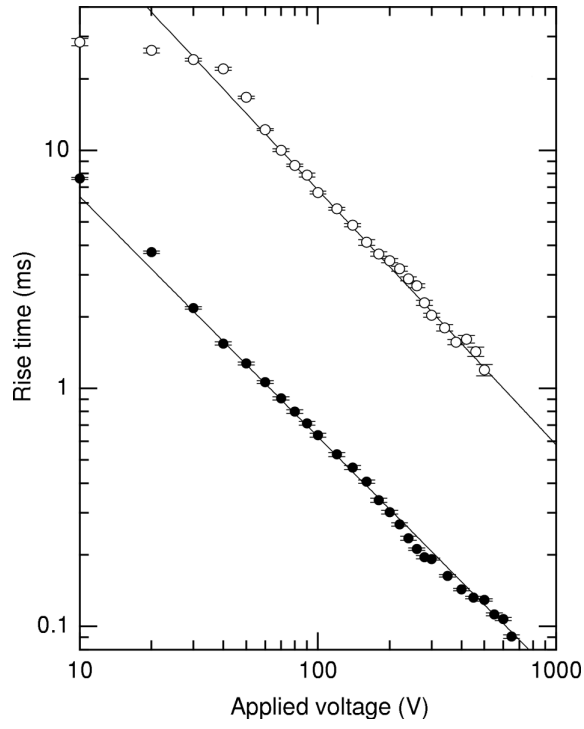

Figure 4
The observed rise time of the multigrid ion chamber (closed circles) as a function of the applied voltage. The result for the three-grid ion chamber is shown by open circles for comparison. The solid lines show the best-fit functions.

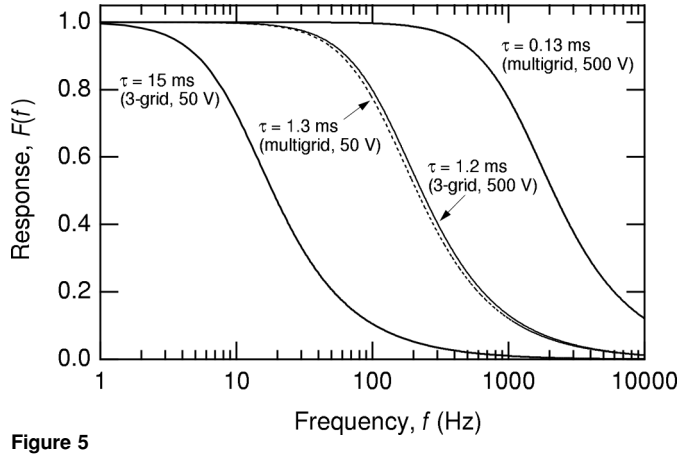

Figure 5
The frequency response of the fluorescent ion chambers. The curves were calculated for different output response times, τ = 15, 1.2, 1.3 and 0.13 ms, which correspond to the three-grid detector used at 50 and 500 V, and the multigrid detector at 50 and 500 V, respectively.

For τ = 15 ms (three-grid at 50 V), the response will be 70% at 10 Hz and decrease to only 25% at 40 Hz, which is the typical frequency at which we perform the helicity-modulation XMCD measurements. If a voltage of 500 V is applied to the three-grid detector (τ = 1.2 ms), a response higher than 95% is obtainable at 40 Hz. However, the output signal was found to be noisy at an applied voltage higher than 200 V owing to some transient discharge inside the chamber. Therefore, the three-grid detector operated at 500 V is of no practical use.

For the multigrid ion chamber, the desirable response is obtainable at a lower applied voltage: the frequency response of the multigrid detector at 50 V (τ = 1.3 ms) is comparable with the three-grid detector operated at 500 V. As shown by the curve for 500 V (τ = 0.13 ms), a higher applied voltage allows a faster response to high frequency. The response at 40 Hz is 100%, which is sufficient for the X-ray modulation spectroscopy presently established. Furthermore, the multigrid detector can operate at 1 kHz with a reasonable amplitude response of 75%. This compatibility to high frequency leads to further improvement of the signal-to-noise ratio of the X-ray modulation spectroscopy using faster modulation.

5. Conclusion

We have developed a new fluorescent ion chamber with 17 grids and a 5 mm grid separation. The rise/fall time of the detector is shortened by more than one order of magnitude compared with the existing three-grid ion chamber. The available response time is as fast as 0.1 ms. The multigrid detector shows sufficiently fast response for the X-ray modulation spectroscopy at 40 Hz. In addition to the high performance in the cyclic mode, the multigrid detector can operate in a conventional d.c. mode, in which the detector shows better linearity owing to the higher electric field between grids. We have already performed a preliminary experiment of fluorescence XMCD in the helicity-modulation mode using the multigrid detector. The compatibility to higher frequency leads to the feasibility of fluorescent XMCD experiments with higher sensitivity in diluted magnetic materials as well as magnetic thin films/multilayer systems, using the helicity modulation in the kHz range.

The authors are grateful to Dr Masayo Suzuki for fruitful discussions. This work was supported by a Japanese Government Grant for Common Use of the Synchrotron Radiation Facility.

References

Kawamura, N., Yamamoto, T., Maruyama, H., Harada, I., Suzuki, M. & Ishikawa, T. (2001). *J. Synchrotron Rad.* **8**, 410–412.
Knoll, G. F. (1989). *Radiation Detection and Measurement*, 2nd ed., pp. 149–157. New York: Wiley.
Lytle, F. W., Greegor, R. B., Sandstrom, D. R., Marques, E. C., Wong, J., Spiro, C. L., Huffman, G. P. & Huggins, F. E. (1984). *Nucl. Instrum. Methods*, **226**, 542–548.
Maruyama, H. (2001). *J. Synchrotron Rad.* **8**, 125–128.
Stern, E. & Heald, S. (1979). *Rev. Sci. Instrum.* **50**, 1579–1582.
Suzuki, M., Kawamura, N. & Ishikawa, T. (2000). *Proc. SPIE*, **4145**, 140–149.
Suzuki, M., Kawamura, N. & Ishikawa, T. (2001). *Nucl. Instrum. Methods A*, **467/468**, 1568–1571.
Suzuki, M., Kawamura, N., Mizumaki, M., Urata, A., Maruyama, H., Goto, S. & Ishikawa, T. (1998). *Jpn. J. Appl. Phys.* **37**, L1488–L1490.
Suzuki, M., Kawamura, N., Mizumaki, M., Urata, A., Maruyama, H., Goto, S. & Ishikawa, T. (1999). *J. Synchrotron. Rad.* **6**, 190–192.
Uemoto, S., Maruyama, H., Kawamura, N., Uemura, S., Kitamoto, N., Nakao, H., Hara, S., Suzuki, M., Fruchart, D. & Yamazaki, H. (2001). *J. Synchrotron Rad.* **8**, 449–451.